Measurement of the drift of a droplet due to the presence of a plane

Jeffrey R. Smart and David T. Leighton Jr.

Citation: Physics of Fluids A **3**, 21 (1991); doi: 10.1063/1.857856
View online: http://dx.doi.org/10.1063/1.857856
View Table of Contents: http://scitation.aip.org/content/aip/journal/pofa/3/1?ver=pdfcov
Published by the AIP Publishing

Measurement of the drift of a droplet due to the presence of a plane

Jeffrey R. Smart and David T. Leighton, Jr.
Department of Chemical Engineering, University of Notre Dame, Notre Dame, Indiana 46556

(Received 16 February 1990; accepted 6 September 1990)

The drift of a deformable droplet of low viscosity (viscosity ratio $\lambda = 0.08$) in a Couette device is examined. The drift is measured both in the plane of shear (due to the rigid outer bounding wall of the Couette device) and also normal to the plane of shear (due to the upper bounding stress-free surface). A general relationship between normal stresses induced by the deformation of a droplet in an arbitrary shear flow and the leading-order drift normal to rigid and stress-free plane surfaces is described theoretically. This relationship is consistent with previous theoretical predictions for droplet migration in shear flows, and is used to compare results from the drift measurement experiments with first-order deformation theories. The measured drift velocities are in reasonable agreement with the theory of Schowalter *et al.* [J. Colloid Interface Sci. **26**, 152 (1968)].

I. INTRODUCTION

A droplet of one fluid immersed in a second immiscible fluid that is undergoing shear will deform. Taylor[1,2] first studied the deformation of a droplet in simple and extensional shear flows. Taylor's theoretical and experimental investigation has been developed further by a number of researchers who have explored the effects of the curvature of shear flows and who have extended the investigations to higher order in the capillary number. Recent reviews of these investigations include those by Rallison[3] and Acrivos.[4]

A droplet of fluid immersed in a simple shear will produce a disturbance velocity. In the absence of deformation the disturbance velocity will be symmetric, and the droplet will not drift normal to a bounding surface in the limit of low Reynolds number. If the droplet deforms, however, then the disturbance velocity will be asymmetric, and the droplet may drift relative to a bounding plane.

The drift of a droplet of arbitrary viscosity normal to the bounding walls of a Couette viscometer has been predicted theoretically by Chaffey *et al.*[5] who found that the droplet would drift away from the walls and toward the center of the Couette gap. Qualitative confirmation of this result was provided by Karnis and Mason,[6] whose experiments supported the theoretical prediction that the drift velocity of a droplet decreases inversely with the square of the distance between the droplet and a bounding wall. Karnis and Mason[6] found that the cube of the distance between the droplet and the wall grew linearly in time (as would be expected from the inverse square dependency of velocity on distance from the wall) and that the drift velocity was an increasing function of the capillary number. These investigators, however, were unable to obtain quantitative agreement between the experimentally measured drift velocities and theoretical predictions. The theoretical prediction of droplet drift has been extended by Chan and Leal,[7] who accounted for the effect of curvature of the flow field in a Couette device having a finite gap width to device radius ratio, and who also explored the effects of non-Newtonian second-order suspending fluids. In later experiments, Chan and Leal[8] measured the trajectories and equilibrium radial position of droplets in a Couette device, and found qualitative agreement with their order capillary number theory.

In addition to resulting in drift normal to a bounding plane, the deformation of droplets also gives rise to non-Newtonian shear stresses in an emulsion. Batchelor[9] showed that the bulk shear stress in a dilute emulsion is simply the sum of the individual contributions of the droplets to the shear stress. Schowalter *et al.*[10] used this approach to calculate the shear stress (to first order in the capillary number) of an emulsion at infinite dilution of droplets of arbitrary viscosity when the emulsion was subjected to linear shear flow. These results have been extended to time-dependent flows by Frankel and Acrivos.[11] Of course, all of the theories predicting the rheology of emulsions from the behavior of individual droplets will be valid only at infinite dilution. For higher concentrations droplet interactions must be taken into account, which has not yet been done.

In this paper we will examine the subject of droplet deformation and migration from both theoretical and experimental viewpoints. In Sec. II, we present results that directly relate the drift velocity of a droplet to the rheological behavior of an emulsion at infinite dilution. While the drift velocities obtained in this manner are similar to previous theoretical results, we have developed a particularly convenient and general relationship between drift velocity and rheological properties. In Sec. III, we describe experiments in which we measure the drift velocity of a droplet normal to the rigid walls (drift in the plane of shear) of a Couette viscometer. In these experiments we systematically examine the effects of capillary number on the migration velocity of a droplet of lower viscosity than the suspending fluid. In addition, we also examine the drift of a droplet normal to the upper bounding stress-free surface; that is, drift normal to the plane of shear. This has not been previously measured. In Sec. IV, we compare our experimental results to theoretical predictions of drift velocities. In Sec. V, we summarize our results and discuss how nonzero normal stress differences are, in general, related to migration in emulsions and suspensions and also how these normal stress differences may lead to nonuniform concentration distributions. In particular we will apply our results to the case of concentrated suspensions

 0899-8213/91/010021-08$02.00

of rigid spheres in which nonzero normal stress differences have been observed.

II. DRIFT OF A STRESSLET DUE TO THE PRESENCE OF A PLANE

Any particle suspended in a creeping shear flow will give rise to some disturbance velocity. The far field of this disturbance velocity is uniquely defined by a stresslet, S_{ij}, such that (repeated indices imply summation)

$$u_i = (-3/8\pi\mu)S_{jk}(x_i x_j x_k/r^5), \tag{1}$$

in which we follow the nomenclature of Batchelor.[9] Note that the stresslet is both symmetric ($S_{ij} = S_{ji}$), and traceless ($S_{ii} = 0$). In a flow bounded by a plane, the disturbance velocity produced by a droplet will not satisfy boundary conditions on the surface of the plane. As a consequence, we must introduce a reflection to this disturbance velocity such that the sum satisfies the appropriate boundary conditions. To leading order for droplets far from the plane, the drift velocity induced by the presence of the plane is simply that of its corresponding stresslet—the reflection velocity of the stresslet evaluated at the position of the droplet. For droplets of finite size such that a/h (where a is the characteristic radius of the droplet and h is its distance from the plane) is not vanishingly small, it is necessary to consider higher-order reflections. Such calculations have been performed by Shapira and Haber;[12,13] however, in this paper we will consider only the leading-order term due to the stresslet.

The most general relationship for the drift velocity of a stresslet S_{jk} due to a plane specified by the unit normal n_i is given by[14]

$$u_i^* = S_{jk} n_k (\alpha_1 \delta_{ij} + \alpha_2 n_i n_j), \tag{2}$$

where we have made use of the facts that the drift velocity u_i must be linear in the stresslet S_{jk} and that S_{jk} is both symmetric and traceless. The constants α_1 and α_2 remain to be determined and will be different for the two boundary conditions being considered; that is, the no-slip condition of a rigid wall and the perfect slip condition of a free surface.

Let us consider first the case of a rigid wall. We may determine the coefficients α_1 and α_2 by employing stresslets that are conveniently oriented with respect to the plane. While the image system of the stresslet in a rigid plane has not been determined, Blake[15] provides the image system of a Stokeslet, and this can easily be used to obtain the image system of a stresslet. In this manner, we obtain[14]

$$\alpha_1 = (-1/8\pi\mu)(3/4h^2), \tag{3a}$$

$$\alpha_2 = (-1/8\pi\mu)(3/8h^2), \tag{3b}$$

where h is the distance between the stresslet and the plane. From Eq. (2) the drift of an arbitrary stresslet due to the presence of a rigid wall is thus given by

$$u_i^* = S_{jk} n_k \left(\frac{-1}{8\pi\mu}\frac{3}{4h^2}\right)\left(\delta_{ij} + \frac{1}{2} n_i n_j\right). \tag{4}$$

For the case of a free surface, the problem is actually much simpler, since the image of a stresslet is its reflection in the plane. As a consequence, if we again use two conveniently oriented stresslets, we find that the corresponding coefficients β_1 and β_2 are given by

$$\beta_1 = 0, \tag{5a}$$

$$\beta_2 = (-1/8\pi\mu)(3/4h^2), \tag{5b}$$

which yields the following for the drift velocity due to the presence of a stress-free surface:

$$u_i^* = S_{jk} n_k [(-1/8\pi\mu)(3/4h^2)] n_i n_j. \tag{6}$$

Thus the drift normal to a free surface is given by

$$u_i^* n_i = S_{jk} n_j n_k [(-1/8\pi\mu)(3/4h^2)] \tag{7}$$

and that normal to a rigid wall by

$$u_i^* n_i = S_{jk} n_j n_k [(-1/8\pi\mu)(9/8h^2)]. \tag{8}$$

We see that for both boundary conditions the drift velocity normal to a plane is proportional only to the diagonal component of the stresslet normal to the plane (i.e., drift normal to the plane $x_3 = 0$ is proportional to S_{33}). We also note that the drift velocity of a couplet—a point source of angular momentum—normal to a plane is identically zero. This is a consequence of symmetry and may be easily verified by examination of the image system for a couplet provided by Blake and Chwang.[16]

To complete the connection between the rheological properties of a dilute emulsion and the drift velocities of the individual stresslets (droplets) due to a plane wall, we use Batchelor's[9] relationship for the contribution of particles to the bulk shear stress σ^p_{ij}:

$$\langle S_{ij} \rangle = (1/n)\sigma^p_{ij} = \sigma^p_{ij}\left(\tfrac{4}{3}\pi a^3/\phi\right), \tag{9}$$

where n is the number density of the suspended droplets, ϕ is the volume fraction of the droplets, a is the radius of an undeformed droplet, and, for a dilute emulsion where the droplets do not interact with each other, $\langle S_{ij} \rangle$ is just the stresslet which would be obtained for an isolated droplet. Hence the drift of the droplets in a dilute emulsion normal to a rigid wall is simply given by

$$u_i^* n_i = \sigma^p_{jk} n_j n_k \left(\frac{\frac{4}{3}\pi a^3}{\phi}\right)\left(\frac{-1}{8\pi\mu}\frac{9}{8h^2}\right) \tag{10}$$

and the corresponding drift normal to a free surface is given by

$$u_i^* n_i = \sigma^p_{jk} n_j n_k \left(\frac{\frac{4}{3}\pi a^3}{\phi}\right)\left(\frac{-1}{8\pi\mu}\frac{3}{4h^2}\right), \tag{11}$$

which is proportional to the particle-induced normal stress component in the direction of the plane unit normal. Of course, since this result is strictly valid only for emulsions at infinite dilution, the drift of droplets in more concentrated emulsions will differ from that given by Eqs. (10) and (11). Still, the drift predicted here may be qualitatively correct even at finite concentrations.

III. EXPERIMENT

A. Materials

The drift of an inviscid drop was measured using the Couette device depicted in Fig. 1. The outer cylinder, composed of Plexiglas mounted on an aluminum base, had an inner radius of 11.74 cm, and was machined to a tolerance of $\pm 50\,\mu$m. The inner cylinder was aluminum with a radius of 9.73 cm, resulting in an aspect ratio $(R_0 - R_i)/R_0$ of 0.171. A lower bounding surface was provided by a 0.5 cm thick

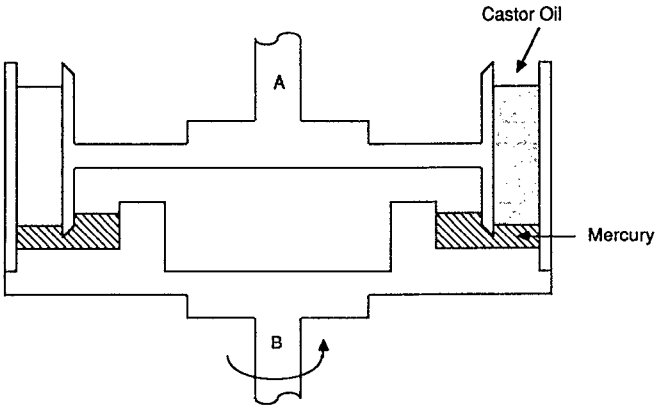

FIG. 1. The Couette device: A, bob; B, cup. The castor oil is confined in the annular region between the bob and cup, supported by a layer of mercury.

layer of mercury. Air provided a stress-free upper surface for the sheared region. The height of the fluid layer in the Couette device was approximately 5 cm. The Couette device was mounted on an R-17 Weissenberg rheogoniometer. The suspending fluid used in the experiments was castor oil, which had a reported density of 0.961 g/cm^3. The viscosity of the suspending fluid was measured as a function of temperature with a Carri-Med controlled-stress rheometer to be

$$\mu = 8.07 \exp[(25 - T)/14.22], \tag{12}$$

where temperature is in °C and viscosity is in poise. The droplet fluid was a mixture of GE silicon fluids (SF-1147, SF-1250) that closely matched the density of the castor oil. The density difference was measured by examining the drift of a 250 μl droplet in quiescent castor oil and was found to be less than 2×10^{-4} g/cm^3. The droplet viscosity was also measured as a function of temperature and was found to be 0.69 P at 25 °C.

B. Procedure

To measure the drift velocity of a droplet normal to the rigid outer wall of the Couette viscometer, a droplet of known volume was injected with a microliter syringe close to the outer wall and shearing was commenced. The radial position of the droplet in the gap was inferred by measuring the period of revolution of the droplet. Using the known velocity profile of a Newtonian fluid in a Couette viscometer and assuming that the droplet followed the fluid flow, we obtained the dimensionless radial position from the following equation:

$$\frac{h}{d} = \frac{1 - [(1 - 1/\kappa^2)/(\tau/\tau_0) + 1/\kappa^2]^{-1/2}}{(1 - \kappa)}, \tag{13}$$

where h is the distance from the outer wall, d is the gap width, κ is the ratio of the inner wall diameter to the outer wall diameter in the Couette device, τ_0 is the period of revolution of the outer cylinder, and τ is the observed period of revolution of the droplet. When the droplet was very close to the wall it is not clear whether it would follow the velocity of the suspending fluid evaluated at the droplet center. However, calculations indicate that the deviation was small enough so that the calculated radial position was not significantly affected.

Drift normal to the free surface was measured by videotaping the droplet as it passed an observation point in the Couette gap. The videotape was later digitized on an IBM PC-AT for analysis. The position of the upper free surface and the location of the center of the droplet were determined using a cursor.

Thermally induced secondary currents were the most significant source of error in these experiments. Because our drift velocities were very small, on the order of 20 μm/sec or smaller, buoyancy-driven secondary currents caused by temperature gradients across the width of the Couette gap could significantly influence the motion of the droplets. For migration away from the rigid wall, the droplet was placed in the vertical center of the Couette gap since the thermal secondary currents are expected to have a minimum component of velocity normal to the walls in this region. In the experiments observing migration away from the upper free surface of the Couette viscometer, the droplets were placed in the radial center of the gap, where vertical currents are likely to be minimized.

The influence of secondary currents was particularly pernicious for the free-surface migration experiments because, as will be shown later, the migration velocities normal to the free surface were an order of magnitude lower ($\sim$2 μm/sec) than the migration velocities away from the rigid wall. For the free-surface experiments, however, it was possible to estimate the magnitude of the thermally induced secondary currents by examining variations in the period of revolution of the droplets in the Couette device. Thus we were able to reject the data for cases where the effects of thermally induced secondary currents were likely to have been significant. In addition to secondary currents, the sedimentation velocity of the droplet due to the very small density difference between the droplet and the suspending fluid also became significant relative to the free-surface drift at sufficiently large separation distances or at low capillary numbers. The secondary currents and sedimentation velocity limited the lowest capillary number at which the experiments could be performed reliably.

C. Results

1. Deformation

In the droplet migration experiments we wish to measure the drift velocity of a droplet as a function of the capillary number (Ca = $\dot\gamma\mu a/\sigma$, where $\dot\gamma$ is the shear rate, μ is the suspending fluid viscosity, a is the radius of the undeformed droplet, and σ is the interfacial tension between the droplet and the suspending fluid) of the imposed flow. To determine the capillary number, however, it is necessary to measure the surface tension. Unfortunately, surface tension is very difficult to measure for fluids that have the same density, as is the case in these experiments. Also, the surface tension of the droplet–suspending fluid interface may change with time as the surface of the droplet ages. To minimize these and other systematic errors in the experiments, we followed the ap-

proach employed by Chan and Leal[8] and used the order capillary number deformation theory developed by Taylor[2] to measure the surface tension by relating the observed deformation of the droplet to the applied shear stress.

Taylor[2] showed that, for a slightly deformed droplet, a deformation parameter defined as $(L-B)/(L+B)$, where L is length of a deformed droplet and B is its breadth, is given by

$$\frac{L-B}{L+B}=\frac{1}{\sigma}(\dot{\gamma}\mu a)\left(\frac{\frac{19}{16}\lambda+1}{\lambda+1}\right). \tag{14}$$

We measured the deformation of a 10 μl droplet using a video camera and a mirror mounted at a 45° angle to the plane of shear. The droplet was centered both radially and vertically in the gap; the local shear rate was determined from the equations for shear rate in a Couette device of finite gap width. The image recorded on videotape was digitized, and points on the perimeter of the digitized image were fitted to an ellipse, which is the projected shape of a slightly deformed droplet. The results of these experiments are given in Fig. 2. The surface tension is the inverse of the slope of the fitted line, and was 2.36 dyn/cm.

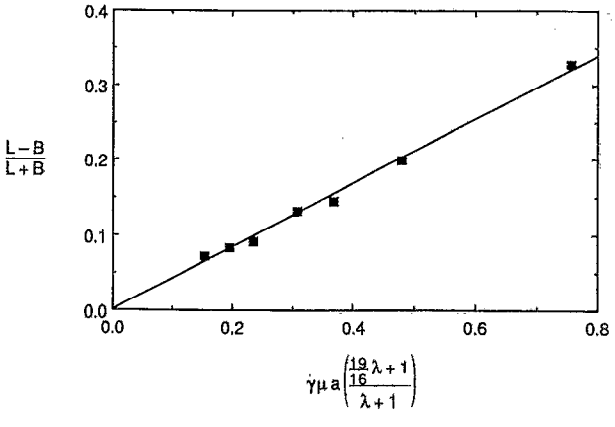

FIG. 2. Droplet deformation versus flow parameters. The inverse of the slope yields the surface tension, which was 2.36 dyn/cm.

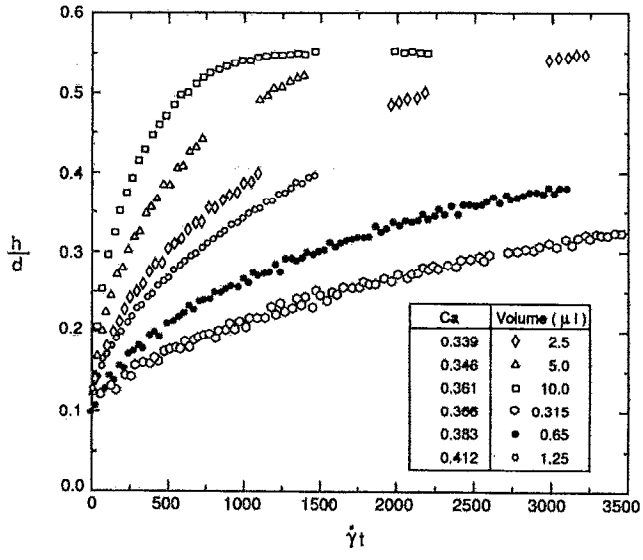

FIG. 3. Dimensionless radial position of droplets in the Couette gap versus dimensionless time for constant capillary number. The droplet position is measured from the outer wall; $h/d=0.5$ corresponds to the center of the gap.

2. Drift normal to a rigid wall

We began our investigations of drift normal to a rigid wall by performing a series of experiments in which the drift of droplets of different volumes was measured. The droplet volume to shear rate ratio was varied so that the capillary number of each of the experiments was approximately constant. In Fig. 3 we plot the dimensionless radial position of the droplet in the gap (h/d) as a function of dimensionless time ($\dot{\gamma}t$), and we find that the velocity of a droplet increases with droplet volume. Note that for the largest droplet (10 μl) the equilibrium position at the center of the gap agreed with that obtained by Chan and Leal.[8]

Since the drift velocity is inversely proportional to the square of the distance between the droplet and the wall, we expect that a plot of the cube of distance from the wall (rendered dimensionless with the radius of a spherical drop of equivalent volume) versus dimensionless time will yield a straight line, as was found by Karnis and Mason.[6] Plots of $(h/a)^3$ vs $\dot{\gamma}t$ are given in Fig. 4 for experiments in which the capillary number was approximately constant but the droplet volume was varied by a factor of 30. Variations in the capillary number in these experiments were due to temperature-induced changes in fluid viscosity. We found that the dimensionless trajectories of the droplets overlaid each other as would be expected since the capillary number was approximately constant for these experiments.

In Fig. 5 we present the measured trajectories of droplets for different capillary numbers having a volume of 1 μl.

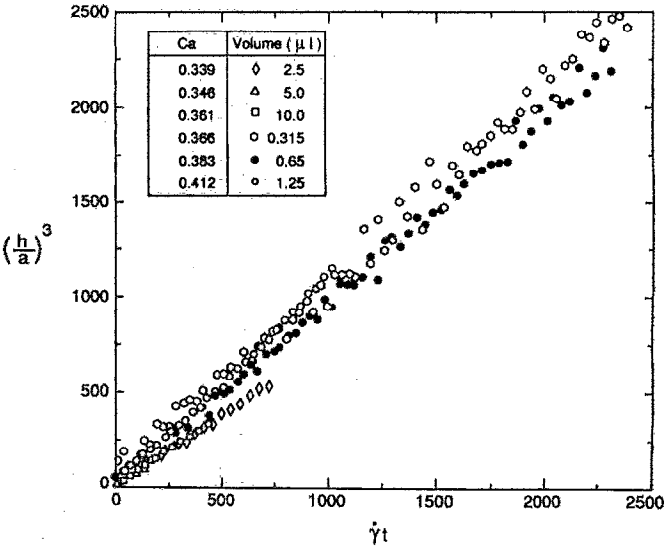

FIG. 4. The cube of the distance from the outer Couette wall to the droplet as a function of dimensionless time for capillary number held approximately constant.

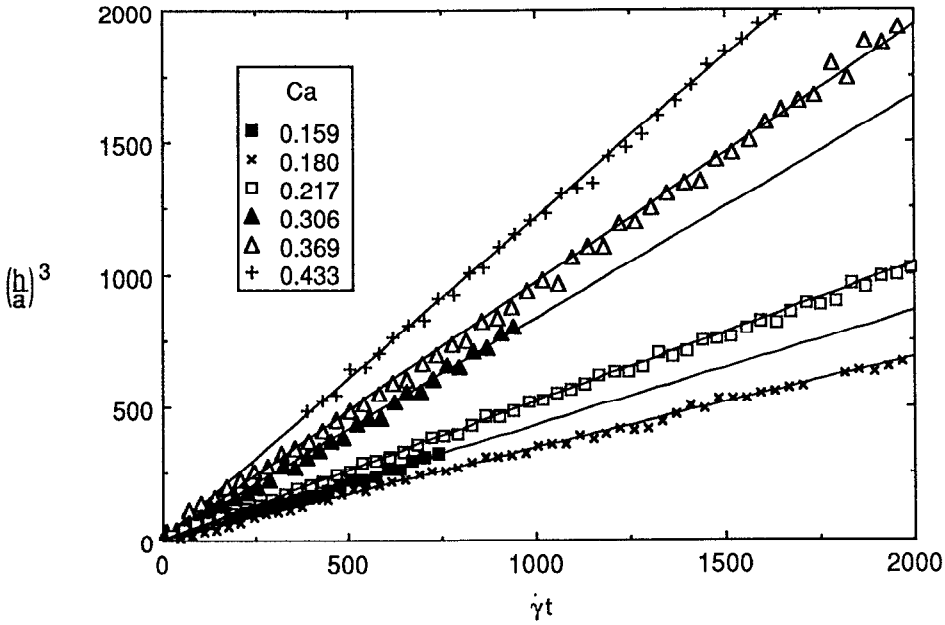

FIG. 5. The cube of the distance between the outer Couette wall and the droplet as a function of dimensionless time for 1 μl droplets at different capillary numbers.

Note that the slopes of the plots of $(h/a)^3$ versus dimensionless time increase as the capillary number increases. This is as expected: since the droplets are more deformed at higher capillary numbers, the drift velocity should increase. In plotting the slopes of these lines as a function of capillary number (Fig. 6), we find that the drift velocity increases linearly in capillary number, as expected from the order capillary number deformation theory. The vertical line in Fig. 6 is the capillary number at which droplet breakup occurred, and the inclined line is the theoretical prediction, which will be discussed in the next section.

The expectation that $(h/a)^3$ grows linearly in time is obtained by only considering the contribution of the first reflection to the drift velocity of the droplet. This will be strictly valid only as h/a becomes large. For small values of h/a it is necessary to consider higher-order reflections. We may obtain information about these higher-order terms by examining the drift velocity for small values of h/a. In Fig. 7 we have plotted the observed trajectory together with the limiting far-field linear trajectory for several capillary numbers for drift normal to the outer Couette wall. Note that for the highest capillary numbers (close to droplet breakup) the deviation from the linear relationship is quite large and persists to values of $h/a \approx 8$. In contrast, at smaller capillary numbers the linear relationship is preserved down to $h/a \approx 2$. In all cases the far field was used to calculate the drift velocity used in Fig. 6.

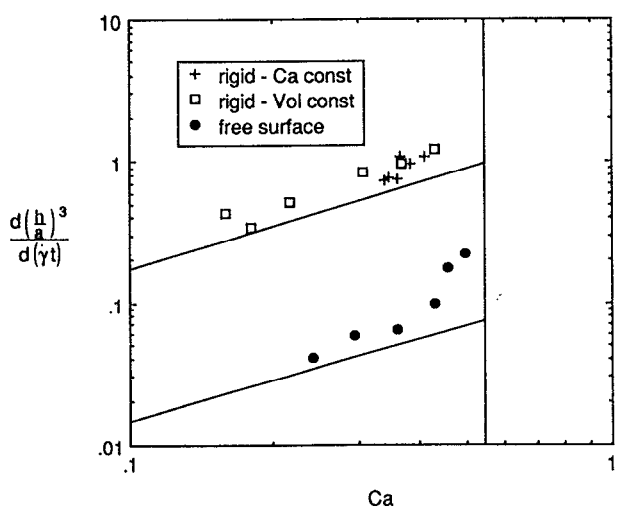

FIG. 6. Slope of $(h/a)^3$ versus dimensionless time as a function of capillary number for both drift away from the upper stress-free surface and drift away from the outer wall of the Couette device. The plotted symbols are experimental observations, the inclined lines are the theoretical predictions, and the vertical line corresponds to droplet breakage.

We have also neglected the contribution of the second wall of the Couette device in calculating the drift velocity. Because of the inverse square dependence of the drift velocity on distance from the wall, we expect the contribution of the second wall relative to the first to be of $O[h^2/(d-h)^2]$, where d is the gap width; thus, the second wall may be neglected provided this parameter is small. In our experiments, however, we found that the linear relationship was preserved out to values of $h^2/(d-h)^2$ as great as 0.4 (Fig. 4), although the larger droplets would eventually achieve some steady position as was described earlier. The velocities used in Fig. 6 were estimated from droplet positions in the outer third of the Couette gap.

3. Drift normal to a free surface

Droplets were found to drift away from both the upper and lower interfaces. We conducted drift measurements only normal to the upper air–castor oil interface, however, since the interfacial shear stresses are much lower here than at the mercury–castor oil interface. In Fig. 8 we plot the drift

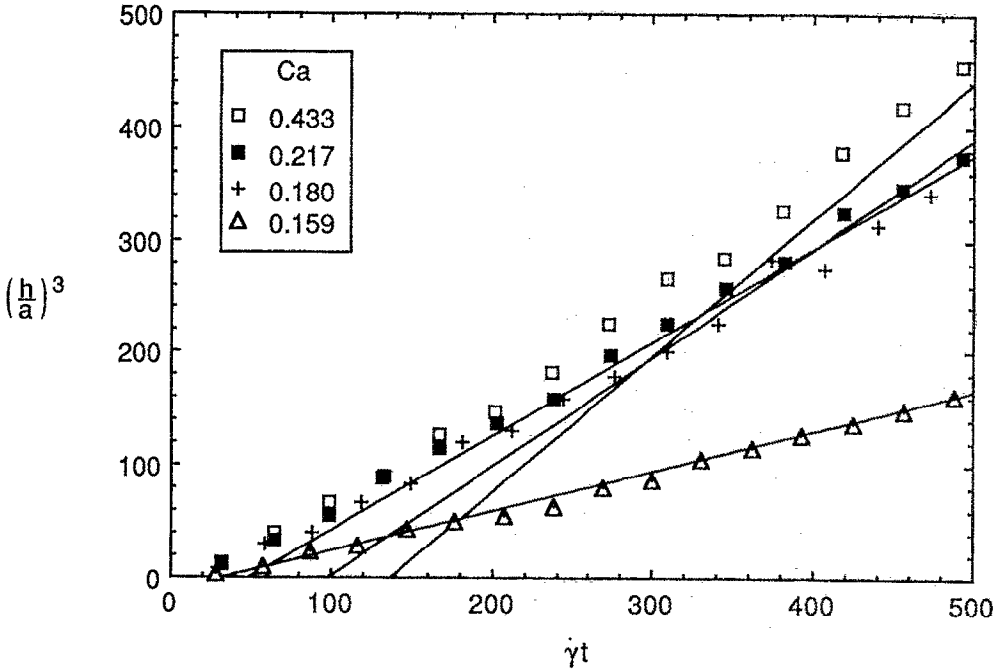

FIG. 7. Near-field drift away from the outer Couette wall. The lines represent the limiting trajectories for large h/a. Lines with smaller horizontal intercepts correspond to smaller capillary numbers.

trajectories $(h/a)^3$ versus dimensionless time for each of the capillary numbers studied. Note that these velocities are an order of magnitude lower than the velocities observed for drift normal to the rigid walls of the Couette device. In Fig. 6 we plot the dimensionless drift velocity as a function of capillary number. At small capillary numbers the velocity is proportional to Ca, as expected from first-order deformation theory. However, the drift velocity increases sharply as the critical capillary number is approached. Because the drift velocity normal to the free surface was much smaller than that normal to the rigid wall it was not possible to reliably measure the drift to as large a value of h/a, particularly at low capillary numbers. From the observed linear dependence of $(h/a)^3$ on time shown in Fig. 8, however, it appears that the drift normal to the free surface was less affected by higher-order reflections than that normal to the rigid walls. This is unsurprising due to the weakness of the disturbance velocity normal to the plane of shear, and also to the fact that the droplet deformation occurs primarily within the plane of shear. Still, the measured drift velocity may have been diminished by the close proximity of the free surface.

In addition, we have also neglected the influence of the

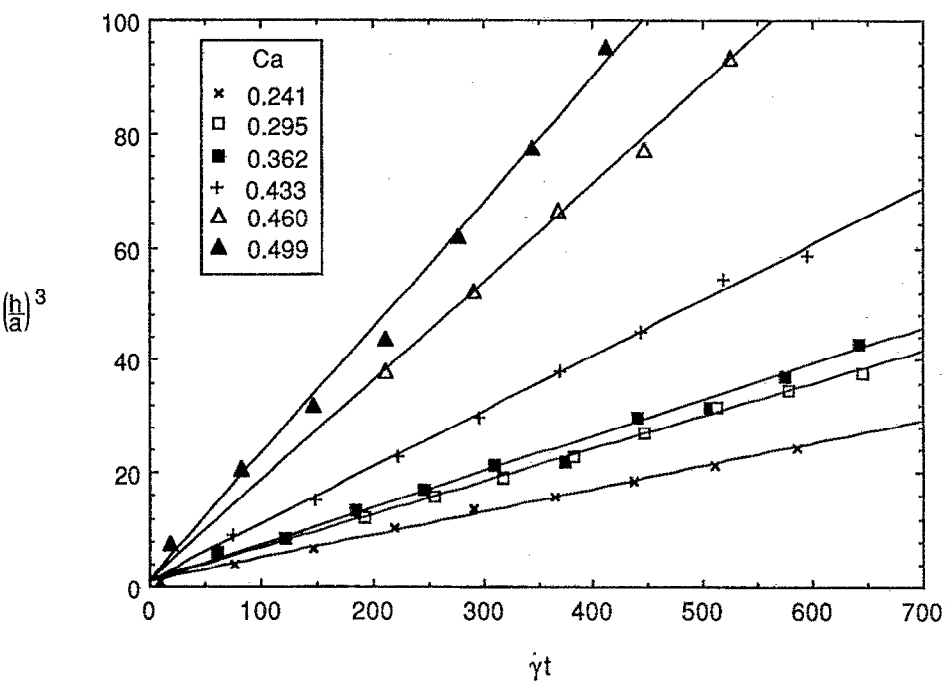

FIG. 8. The cube of the distance between the upper stress-free surface and the droplet as a function of dimensionless time for different capillary numbers.

very slight density difference on the drift velocity. the droplets were very slightly ($<2\times10^{-4}$ g/cm^3) positively buoyant and hence were observed to rise once shearing was terminated after each experiment. Calculations indicate that this sedimentation velocity may have been sufficient to influence the droplet motion at the two lowest capillary numbers studied, although there was no evidence of this in the observed trajectories. The sedimentation velocity was insignificant for higher capillary numbers due to the larger resulting drift velocities.

IV. COMPARISON TO THEORY

The contribution of slightly deformed droplets to the shear stress of an infinitely dilute emulsion undergoing simple shear flow was obtained by Schowalter *et al.*[10] If we consider the shear flow $u_i = \delta_{i1}\dot{\gamma}x_3$, then we are interested in the components of the shear stress σ^p_{33} for drift away from the rigid wall, and σ^p_{22} for drift away from the upper surface. In this coordinate system, these components of the stress are[10]

$$\sigma^p_{33} = \dot{\gamma}\mu\phi\,\mathrm{Ca}\left(\frac{19\lambda+16}{80(\lambda+1)^2}\right)\left(\frac{25\lambda^2+41\lambda+4}{7(\lambda+1)} - (19\lambda+16)\right), \tag{15a}$$

$$\sigma^p_{22} = \dot{\gamma}\mu\phi\,\mathrm{Ca}\left(\frac{19\lambda+16}{80(\lambda+1)^2}\right)\left((-2)\,\frac{25\lambda^2+41\lambda+4}{7(\lambda+1)}\right), \tag{15b}$$

where λ is the ratio of droplet viscosity to suspending fluid viscosity, which for our experiments was 0.083. For this value of λ, the magnitudes of the shear stress components are

$$\sigma^p_{33} = \dot{\gamma}\mu\phi\,\mathrm{Ca}\,(-3.11), \tag{16a}$$

$$\sigma^p_{22} = \dot{\gamma}\mu\phi\,\mathrm{Ca}\,(-0.374). \tag{16b}$$

Using the results of Sec. II where we relate the velocity of the droplets to the rheological properties of the emulsion at infinite dilution, we may obtain an expression for the drift velocity normal to a rigid wall and to a stress-free surface. For the viscosity ratio used in our experiments, these have the following magnitudes:

$$u_i^* n_i = \dot{\gamma}\mu\phi\,\mathrm{Ca}(-3.11)\left(\frac{\frac{4}{3}\pi a^3}{\phi}\right)\left(\frac{-1}{8\pi\mu}\,\frac{9}{8h^2}\right), \tag{17a}$$

$$u_i^* n_i = \dot{\gamma}\mu\phi\,\mathrm{Ca}(-0.374)\left(\frac{\frac{4}{3}\pi a^3}{\phi}\right)\left(\frac{-1}{8\pi\mu}\,\frac{3}{4h^2}\right), \tag{17b}$$

respectively. Note again that the drift normal to the upper free surface is an order of magnitude lower than the drift normal to a rigid wall in this geometry.

By recognizing that the normal velocities in Eqs. (17) (the left-hand sides) can be rewritten as dh/dt, these equations can be integrated to yield

$$(h/a)^3 = 1.75\,\mathrm{Ca}\,(\dot{\gamma}t) + (h/a)^3|_{t=0}, \tag{18a}$$

$$(h/a)^3 = 0.14\,\mathrm{Ca}\,(\dot{\gamma}t) + (h/a)^3|_{t=0}. \tag{18b}$$

These theoretical predictions are compared to the experimental observations in Fig. 6.

The agreement between theory and experiment is quite good, particularly considering that there are no adjustable parameters in the theoretical calculations, except to the extent that we use Taylor's order capillary number deformation theory to calculate the surface tension and hence the capillary number. It is unclear whether the discrepancy between our experimental results and theoretical predictions is due to systematic experimental error (which would not be surprising in view of the difficulty in performing these experiments), to the capillary number in our experiments not being sufficiently small to approach the asymptotic behavior for small deformations, or to the formation of some elastic "skin" on the surface of the droplets. It was not possible to conduct the experiments at smaller capillary numbers because the velocities of thermally driven secondary currents became significant relative to the drift velocities of the droplets.

V. SUMMARY

In this paper we have presented a simple and convenient relationship between observable rheological properties of dilute suspensions and emulsions and the drift of the constituent particles due to the presence of plane interfaces. By examining the drift of droplets normal to both the outer rigid wall of a Couette viscometer and the upper free surface, we have demonstrated reasonable quantitative agreement between these experiments and small deformation theory, and have verified that the magnitude of the stresslet component σ^p_{22} at infinite dilution is an order of magnitude less than the stresslet component σ^p_{33}, as is predicted by the theory.

It is intriguing to explore the implications of this droplet migration to nonuniform concentration distributions in flows of emulsions and suspensions. It has long been known that droplet deformation leads to the migration of droplets to the center of tube flow, for example. Our results suggest that whenever nonzero normal stress differences for a dilute emulsion or suspension are of the type examined here, we may expect the droplets or particles to drift away from the bounding walls, resulting in a nonuniform concentration distribution. This has interesting implications for the case of concentrated suspensions of rigid spheres. Obviously, from the linearity of the governing flow equations, an isolated sphere in a simple shear flow will experience no drift away from the walls, just as was the case for a spherical drop. This is in agreement with the theoretical prediction that a dilute suspension of spheres is Newtonian and hence for a simple shear flow the normal stress differences are zero. In a concentrated suspension, however, the particles making up a suspension tend to form aggregates[17,18] and the suspensions themselves have been observed to exhibit the same normal stress differences that would be expected for a dilute emulsion of droplets undergoing shear flow.[19]

Therefore if we model a concentrated suspension of rigid spheres as a dilute suspension of deformable aggregates and ascribe the observed normal stresses to the deformation of these aggregates, then we would expect that the aggregates would drift away from the walls of a Couette viscometer. This drift could lead to concentration variations in bounded simple shear flows and may account for the deformation of the velocity profile of concentrated suspensions observed in a Couette viscometer by Karnis *et al.*[20] or the

depletion of particles in the near-wall regions of a Couette viscometer indirectly observed by Eckstein[21] for large particle diameter to gap width ratios. Nonzero normal stresses and the resulting concentration inhomogeneities may also occur in other systems such as electrorheological and magnetic fluids under the imposition of external fields. Further work is clearly necessary to determine the importance of this anisotropy-induced migration on concentration profiles in suspensions.

ACKNOWLEDGMENTS

We would like to thank Dr. Jeffrey Kantor for his assistance in determining the deformation of droplets in a shear flow. We are indebted to Mitech Corp. for the donation of the Carri-Med controlled stress rheometer used in this work.

This work was supported by the National Science Foundation.

[1]G. I. Taylor, Proc. R. Soc. London Ser. A **138**, 41 (1932).
[2]G. I. Taylor, Proc. R. Soc. London Ser. A **146**, 501 (1934).
[3]J. M. Rallison, Annu. Rev. Fluid Mech. **16**, 45 (1984).
[4]A. Acrivos, Ann. N.Y. Acad. Sci. **404**, 1 (1983).
[5]C. E. Chaffey, H. Brenner, and S. G. Mason, Rheol. Acta **4**, 64 (1965).
[6]A. Karnis and S. G. Mason, J. Colloid Interface Sci. **24**, 164 (1967).
[7]P. C.-H. Chan and L. G. Leal, J. Fluid Mech. **92**, 131 (1979).
[8]P. C.-H. Chan and L. G. Leal, Int. J. Multiphase Flow **7**, 83 (1981).
[9]G. K. Batchelor, J. Fluid Mech. **41**, 545 (1970).
[10]W. R. Schowalter, C. E. Chaffey, and H. Brenner, J. Colloid Interface Sci. **26**, 152 (1968).
[11]N. A. Frankel and A. Acrivos, J. Fluid Mech. **44**, 65 (1970).
[12]M. Shapira and S. Haber, Int. J. Multiphase Flow **14**, 483 (1988).
[13]M. Shapira and S. Haber, Int. J. Multiphase Flow **16**, 305 (1990).
[14]D. T. Leighton, Jr., Ph.D thesis, Stanford University, 1985.
[15]J. R. Blake, Proc. Cambridge Philos. Soc. **70**, 303 (1971).
[16]J. R. Blake and A. T. Chwang, J. Eng. Math. **8**, 23 (1974).
[17]A. L. Graham and R. B. Bird, Ind. Eng. Chem. Fundam. **23**, 406 (1984).
[18]A. L. Graham and R. D. Steele, Ind. Eng. Chem. Fundam. **23**, 411 (1984).
[19]F. A. Gadala-Maria, Ph.D thesis, Stanford University, 1979.
[20]A. Karnis, H. L. Goldsmith, and S. G. Mason, J. Colloid Interface Sci. **22**, 531 (1966).
[21]E. C. Eckstein, Ph.D thesis, Massachusetts Institute of Technology, 1975.